© 1999 Nature America Inc. • http://neurosci.nature.com

Receptive fields of disparity-selective neurons in macaque striate cortex

Margaret S. Livingstone and Doris Y. Tsao

Department of Neurobiology, Harvard Medical School, 220 Longwood Ave., Boston, Massachusetts 02115, USA
Correspondence should be addressed to M.L. (mlivingstone@hms. harvard. edu)

To identify neuronal mechanisms underlying stereopsis, we characterized interactions between inputs from the two eyes in disparity-selective neurons in macaque V1. All disparity-selective cells showed suppressive interactions between the right and left eyes, and some showed facilitatory interactions. Disparity selectivity was narrower than the receptive-field width and was constant across the receptive field. Such position-invariant disparity selectivity is also found in anesthetized cat V1. Complex cells have been suggested to inherit their disparity selectivity from simple cells with receptive fields mismatched between the two eyes. However, we found no such antecedent disparity-tuned simple cells. We did find disparity-selective cells with some simple-cell characteristics, but surprisingly, they also showed position-invariant disparity selectivity rather than simple linear binocular interactions.

© 1999 Nature America Inc. • http://neurosci.nature.com

When an object is nearer or farther than an observer's fixation point, its images differ in position on the two retinae (**Fig. 1a**); this discrepancy is termed binocular disparity. Stereopsis is the ability to interpret binocular disparity as distance from the observer[1]. Cells whose firing rates vary with binocular disparity have been described in striate and extrastriate visual cortex of cats, monkeys and sheep and in the visual Wulst of the owl[2–14]. Yet neuronal mechanism(s) underlying disparity selectivity remain unclear.

The kinds of disparity selectivity found in primates are throughly characterized[15–17], but no studies have investigated the underlying receptive-field mechanisms. Given that disparity-selective cells are found in primate primary visual cortex (V1) and that V1 is the first level in the retinogeniculocortical visual pathway at which inputs from the two eyes converge, the mechanisms underlying disparity selectivity must be found there.

Most binocular cells in V1 have identical receptive fields in the two eyes[18] and would presumably respond optimally at zero disparity (the fixation plane). It is not clear, however, whether such cells would necessarily be involved in depth perception. We can be more certain that cells responding optimally at nonzero disparities (corresponding to stimuli nearer or farther than the fixation plane) are likely to be involved in depth perception. We therefore consider cells to be disparity tuned only if they are maximally responsive at some nonzero disparity, or if they are narrowly tuned (relative to receptive-field width[15,17]) to zero disparity, acknowledging that these criteria may exclude some zero-tuned cells that actually are involved in stereopsis.

For a cell to respond preferentially to a nonzero disparity, there must be offsets or mismatches between the inputs from the two eyes either to that cell or to its antecedents. Early studies suggested that in disparity-selective cells, the receptive field of one eye is spatially offset from the receptive field of the other eye[4,8]. A receptive-field offset between the eyes would result in a cell with precise disparity tuning only if the receptive fields were small. This is the case for simple cells, which have narrow receptive-field subunits, but not for complex cells, which respond to a bar anywhere over a wider region of visual space, suggesting that disparity selectivity is wired up at or before the complex cell stage. Complex cells are also contrast invariant: they respond similarly to light or dark bars, whereas subregions of receptive fields of simple cells are sensitive to contrast, responding to light bars with excitation and dark bars with inhibition, or *vice versa*. The fact that our perception of binocular disparity depends critically on contrast (we do not perceive depth from a light bar in one eye paired with a dark bar in the other eye) also suggests that disparity selectivity is wired very early, at or before the complex cell stage. More recently, Ohzawa and colleagues proposed that the building blocks for disparity selectivity are simple cells in which the two eyes' receptive fields differ in ON and OFF subunit organization within the receptive field (phase shift), rather than differing in overall receptive-field location (position shift[9,19-21]; **Fig. 1b-d**). Figure 1b shows the expected binocular response map[9] (firing rate as a function of stimulus position in each eye) from a model binocular simple cell with identical receptive fields in the two eyes. This cell shows simple linear summation of the inputs from the two eyes. The two arms of the cross represent responses of each eye alone (response profiles shown along each axis), and the central region represents responses when both eyes were stimulated within the activating region. The diagonal graph above right is the response along the –45° diagonal of the interaction map and shows the disparity tuning of this model cell. Despite the response modulation as a function of disparity, we would not consider this cell to be disparity selective because the tuning is as broad as the width of the receptive field. Figure 1 shows model simple cells with nonzero disparity preference generated by linear binocular interactions between inputs with receptive-field offsets (**Fig. 1c**) or phase shifts (**Fig. 1d**) between the two eyes[19–21].

Ohzawa *et al.*[9,10] used binocular reverse-correlation[20] mapping to look at interactions between the two eyes' inputs to single cells in anesthetized cats. They found that some complex cells showed disparity selectivity that was narrower than the receptive-field

© 1999 Nature America Inc. • http://neurosci.nature.com

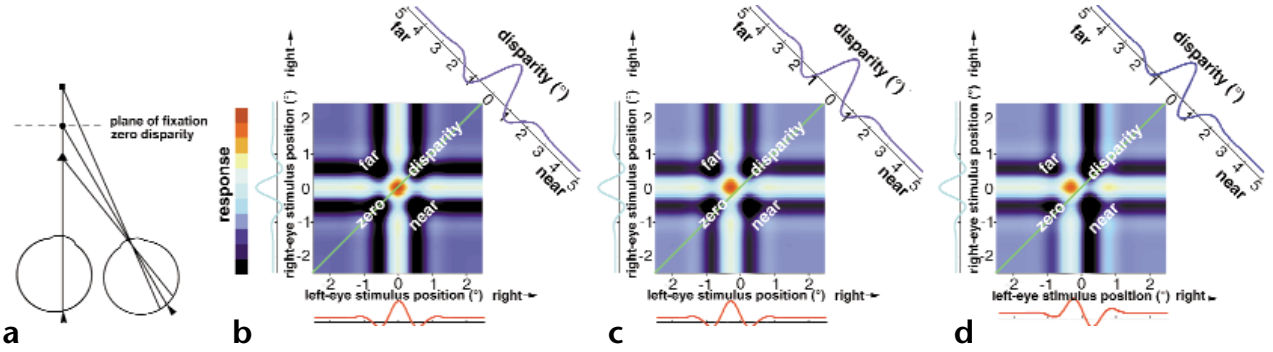

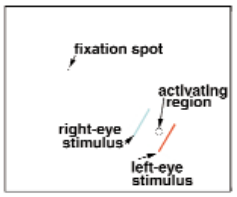

Fig. 1. (a) Objects nearer or farther than the plane of fixation cast images on noncorresponding parts of the two retinae; arrowheads indicate corresponding positions. **(b–d)** Model binocular simple cells showing linear summation of inputs from the two eyes. Receptive fields are mapped in only one dimension in each eye, with OFF responses subtracted from ON responses. In all figures, points on the fixation plane (same retinal location on the two eyes) map onto the +45° diagonal (diagonal green line); isodisparity lines run parallel to that, with near disparities mapping below/right and far disparities above/left. **(b)** Model binocular simple cell with identical receptive fields in the two eyes (not disparity selective). **(c)** Model binocular simple cell preferring far disparities; disparity generated from positional offset of receptive fields in the two eyes. **(d)** Model binocular simple cell preferring far disparities; disparity generated from phase offsets of receptive-field subunits between the two eyes. **(e)** Stimulus configuration used to map binocular interactions in alert monkeys. Pairs of bars, one for each eye, were flashed in a region covering the cell's activating region while the monkey fixated. Responses are mapped as a function of stimulus position in the left (horizontal axis) and right (vertical axis) eyes; positive direction on each axis represents rightward[9,10].

width and constant across the receptive field. That is, these cells showed position-invariant disparity selectivity, and the authors suggested that this kind of cell would be an "ideal disparity detector". However, because their recordings were done in anesthetized, paralyzed cats, the authors could not know the relative position of the two eyes with any accuracy in the spatial range of the binocular interactions, so it could not be determined whether any of their ideal disparity detectors would have preferred non-zero disparities when the eyes were aligned. They proposed that such disparity-tuned complex cells inherit their disparity selectivity from a series of disparity-tuned simple cells.

In this study, we used a similar binocular mapping technique, modified to give high-resolution mapping in the alert monkey (**Fig. 1e**)[23], to generate one-dimensional receptive-field maps in the two eyes and to measure binocular interactions in disparity-selective cells in macaque primary visual cortex. Alert, unanesthesized animals fixate on the monitor screen, allowing precise identification of zero disparity. We found that all cells with non-zero disparity preference, whether simple or complex, exhibited the same disparity preference over the entire range of their receptive fields, and this disparity preference was narrower than the width of the cells' receptive fields.

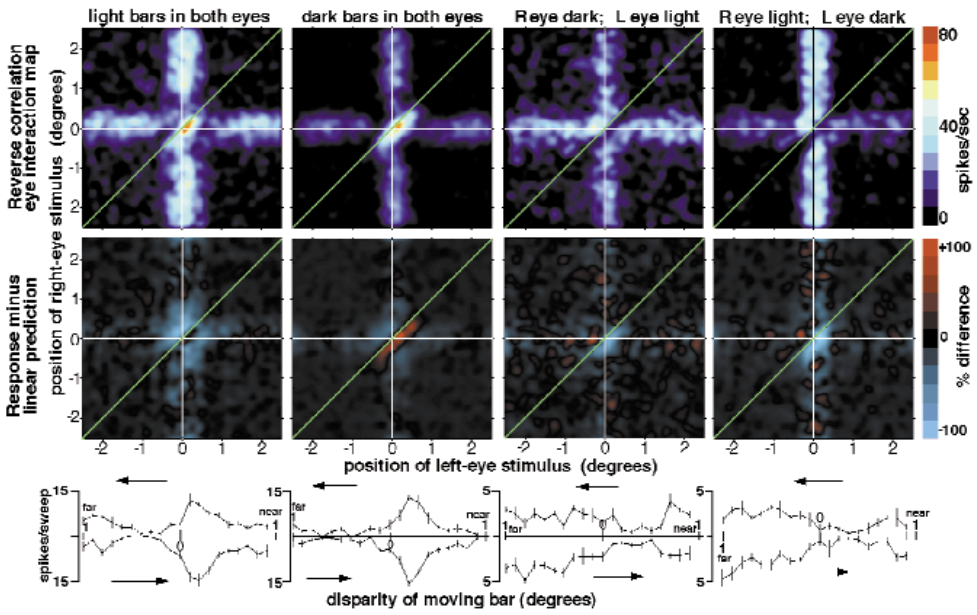

Fig. 2. Responses from a 'tuned near' complex cell. Each column shows results for different stimulus contrasts, as indicated. Top row, reverse-correlation binocular-response maps corrected for eye position at 60 ms before each spike. Middle row, binocular nonlinear interaction maps calculated by subtracting the linear sum of the monocular maps from the actual binocular-response maps; difference is expressed as a fraction of the maximum response for that bar/contrast condition. Bottom row, disparity-tuning graphs generated using a pair of optimal moving bars, one in each eye. This cell had a preferred orientation of 16° clockwise from vertical and a receptive-field eccentricity of 9°. Based on physiological criteria, it was attributed to layer 4B.

© 1999 Nature America Inc. • http://neurosci.nature.com

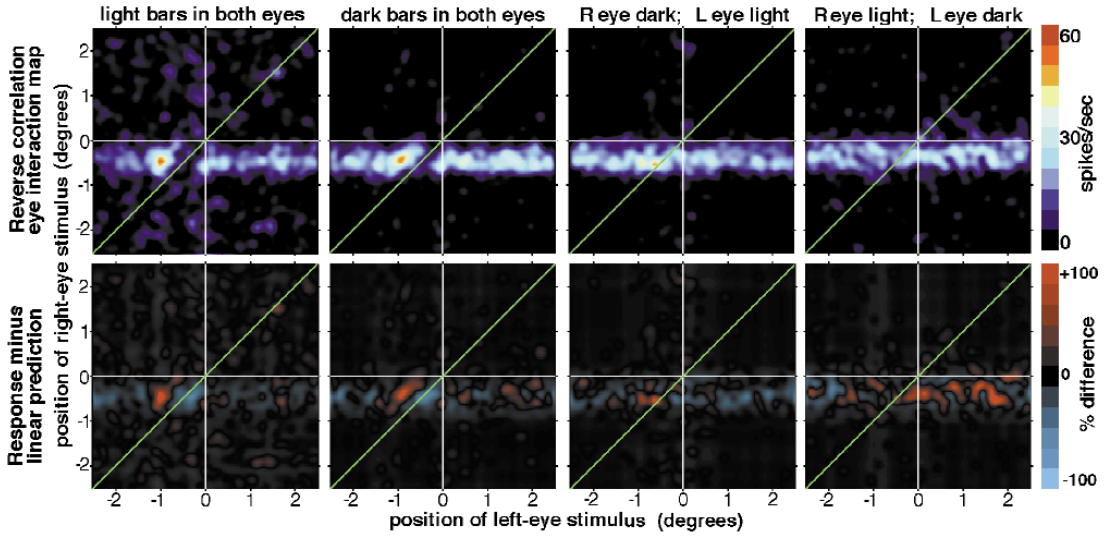

Fig. 3. Reverse-correlation binocular-response maps corrected for eye position (top row) and binocular nonlinear interaction maps (bottom row) at 60 ms before each spike for a 'tuned far' complex cell recorded in alert macaque V1. Conventions as in Fig. 2. Location of right-eye responses below the horizontal center line reflects a stimulus range off-center to the cell's activating region. This cell had a preferred orientation of 10° counterclockwise from vertical and a receptive-field eccentricity of 9°. Based on physiological criteria, the cell was attributed to layer 4B.

Results

We recorded from 42 disparity-selective cells in V1 in 2 alert macaques while the monkeys performed a simple fixation task. We flashed pairs of bars (one visible to each eye) over a region spanning each cell's receptive field, using colored stimuli and colored filters in front of the animal's eyes. We tested both light and dark bars in interdigitated runs. Of these disparity-tuned cells, 17 responded best over either a broad or narrow range of near disparities ('near' or 'tuned near', respectively[15–17]), 13 responded best to far disparities ('far' or 'tuned far'[15–17]), 1 showed a minimum response at zero disparity ('tuned inhibitory'[15–17]) and 11 responded optimally over a relatively narrow range near zero disparity ('tuned excitatory'[15–17]). Twenty-seven nonstereo cells were also mapped for comparison. Even for cells we thought might be simple, we mapped light and dark stimuli independently to avoid any presumption about the receptive-field organization. (Simple cells have spatially segregated light- and dark-excitatory subregions, whereas ON and OFF responses overlap in complex cells[18].)

Binocular interactions in complex cells

Each binocular response map for a disparity-tuned complex cell (top row, first 2 panels, **Fig. 2**) shows a cross-like figure with a diagonal band in the center. Each complex cell was identified by light-bar and dark-bar responses that both mapped to the same region along the stimulus range for each eye. The fact that the region of highest responsiveness was diagonal means that the cell preferred stimuli over a relatively narrow disparity range (about 0.3° wide), peaking at 0.15° near disparity, over an activating region almost 1° wide. That is, the cell showed position-invariant disparity selectivity[9,10]. This cell also showed regions of disparity-selective reduced firing running parallel to the disparity-selective maximum responsiveness. Similar diagonal (position-invariant) isodisparity bands of maximum and/or minimum responsiveness were a feature in all the disparity-tuned cells we mapped. For moving light or dark bar stimuli, this cell also responded best at small near disparities (bottom row).

A second disparity-tuned complex cell is shown in Fig. 3. This cell responded almost exclusively to the right eye when stimulated monocularly, yet showed significant binocular interactions. The binocular response maps (first two panels in the top row) show a region of optimum response to the far side of zero disparity, with a diagonal (position-invariant) band of reduced responsiveness at zero disparity.

To ask how often the binocular interactions were position invariant, we compared the width of the peak binocular interaction along the +45° and –45° diagonals (**Fig. 4**). If the inputs from the two eyes simply summed linearly, and there were no position-invariant interaction, as shown in the three model cells in Fig. 1, the width of the peak should be the same along the +45° and –45° diagonals. Figure 4 shows that the disparity-selective

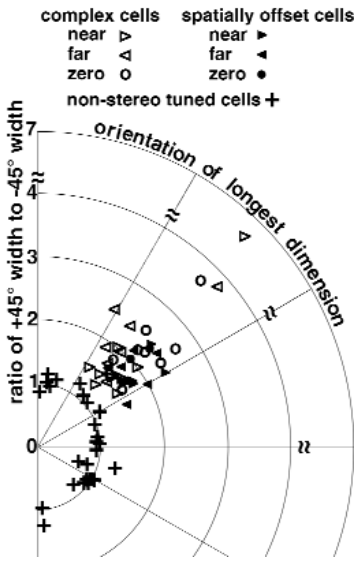

Fig. 4. Elongation ratio and angle of the peak region in binocular response maps for all disparity-tuned cells in this study in addition to 27 non-stereo cells. The distance of each point from the origin indicates the ratio of the width along the +45°diagonal to the width along the –45° diagonal of the peak region in the binocular response map. The angle of each point indicates the angle of the longest dimension of the peak region. Both values were calculated from a contour at 75% peak height.

© 1999 Nature America Inc. • http://neurosci.nature.com

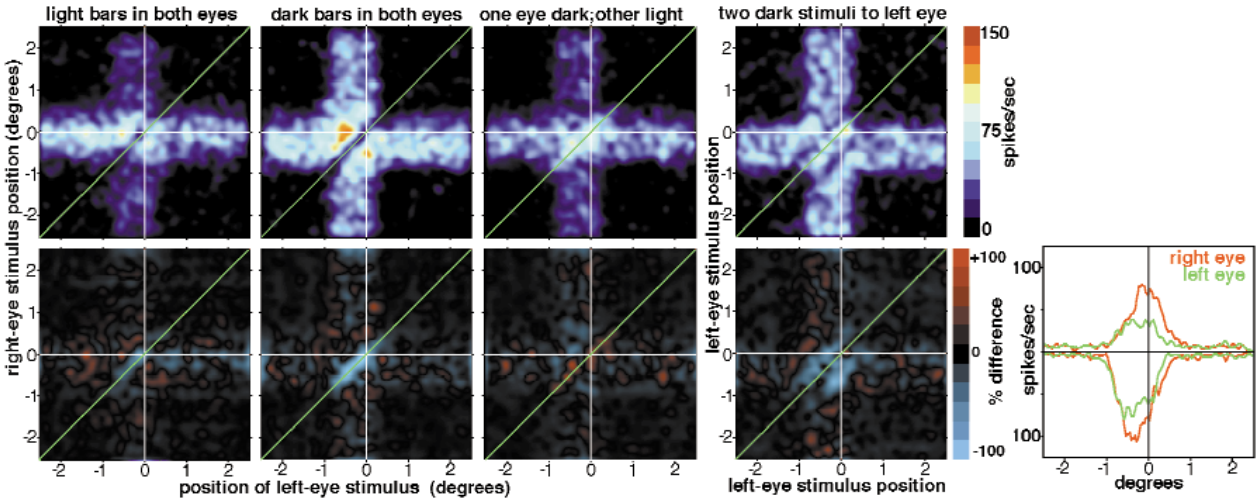

Fig. 5. Reverse-correlation binocular-response maps corrected for eye position and binocular non-linear interaction maps for a 'tuned inhibitory' cell. Conventions as in Fig. 2. The first two panels in the top row show the dark and light-bar binocular-response maps; the third shows the averaged response map for both anticorrelated stimulus conditions. The last panel in the top row shows the response map for two dark bars presented simultaneously to the left eye alone as a function of bar positions. The bottom row shows the corresponding binocular non-linear interaction maps. The bottom right panel shows the averaged light-bar position/response histograms (graphed above the horizontal line) and the averaged dark-bar position/response histograms (graphed below horizontal line) for both eyes. This cell had a receptive-field eccentricity of 9.6°.

cells all had binocular-response peaks that were longer along the +45° diagonal than along the –45° diagonal (ratios all >1).

We considered cells to be disparity tuned only if they showed a nonzero disparity preference or if they showed a disparity selectivity that was narrower than the receptive-field width. Thus in the cells preferring zero disparity, the peak of the binocular response map should be elongated along the +45° diagonal. However, the 'near' and 'far' cells, which were selected not for the narrowness of their disparity tuning, but only for the peak location, also showed diagonally elongated (position-invariant) binocular-interaction peaks. The nonstereo cells had peaks that tended to be round rather than elongated in random directions.

To explore the nature of the binocular interactions, we compared the binocular response maps to the simple linear sum of the monocular responses. The second row of panels in Figs. 2 and 3 show maps of the difference between the actual binocular responses and the linear prediction based on monocular responses, corrected for background firing rate. We refer to such difference maps as 'nonlinear binocular interaction maps' because they reflect only the nonlinear binocular interactions. For the cell in Fig. 2, the light-bar, position-invariant, disparity selectivity seems to be determined largely by suppressive interactions at non-optimal disparities. For dark-bar stimuli, the disparity tuning arises both from disparity-selective facilitation and suppression. Note that the term 'suppression' is used to indicate a firing rate that is below the sum of the monocular responses and implies no specific synaptic mechanisms. The nonlinear interaction maps for the cell in Fig. 3 show that its disparity selectivity is generated by both binocular facilitation and suppression.

Some disparity-tuned cells in cat and monkey V1 show inverted disparity tuning when tested with stimuli of opposite contrast in the two eyes (anticorrelated stimuli)[9,10,24]. This result is consistent with the idea that the monocular inputs to the antecedent simple cells have some kind of center/surround or lateral inhibitory structure. Binocular responses to anticorrelated stimuli for the cell in Fig. 2 (third and fourth panels, top row) do show inverted maps within the binocular interaction region; that is, they show a position-invariant band of suppression at the same disparity at which the correlated stimuli (first two panels) produced the strongest responses. The cell in Fig. 3, on the other hand, showed diminished disparity selectivity but no clear inverted disparity tuning.

Cells with spatially offset light and dark subregions

A third disparity-tuned cell, shown in Fig. 5, introduces a problem we had in identifying some cells as either simple or complex. This cell was 'tuned inhibitory'. The nonlinear interaction maps in the lower panels show that this tuned inhibitory disparity selectivity was generated predominantly by suppressive binocular interactions at zero disparity. The third panels in both rows show that this cell had inverted (tuned excitatory) binocular responses to anticorrelated stimuli. The far right panel in the bottom row shows receptive-field response profiles for the right (red) and left (green) eyes for light (upward going) and dark (downward going) stimuli. For both eyes, the light-bar excitatory response region was located slightly to the right of the dark-bar excitatory region. Yet this cell is not simple, as it shows a position-invariant band of suppressive binocular interaction, and the responses for the left eye are mostly overlapping. If, instead of mapping light and dark stimuli independently, we had subtracted the dark-stimulus responses from the light-stimulus responses, as is commonly done, this cell would have seemed to have spatially segregated ON and OFF subregions.

Figure 5 (fourth column) shows this cell's responses to pairs of bars presented simultaneously to the left eye alone, mapped as a function of both stimulus locations. This map shows a diagonal band of facilitation, corresponding to occasions when the two stimuli were presented very closely or superimposed (yielding a single stimulus of double brightness). Flanking the band of high responsiveness are parallel diagonal bands of reduced responsiveness. Similar two-bar interactions are observed in complex cells in the cat[25] and were interpreted as reflecting the subunit structure of antecedent simple cells, each having lateral inhibitory flanks and

© 1999 Nature America Inc. • http://neurosci.nature.com

© 1999 Nature America Inc. • http://neurosci.nature.com

receptive-field locations spatially offset from one another.

Disparity tuning in complex cells could be generated either directly from monocular inputs with systematic offset or mismatch in their receptive fields, or could be inherited from a series of antecedent disparity-tuned simple cells. These simple cells could create disparity tuning either by phase offsets of the simple-cell subregions, or by positional offsets of their entire receptive fields[9,19–21] (**Fig. 1c** and **d**). As models suggest that inputs from at least four simple cells are required to make up a complex cell with position-invariant disparity selectivity[10], we expected to find a lot of disparity-selective simple cells in V1. Despite mapping every disparity-tuned cell we recorded from, we found not one disparity-tuned simple cell whose eye-interaction map could be predicted as a simple sum (or squared or rectified sum) of its monocular receptive fields. We did, however, record some disparity-tuned cells that showed some characteristics of simple cells: ten disparity-tuned cells showed nearly or completely non-overlapping light and dark-bar response regions, and six cells

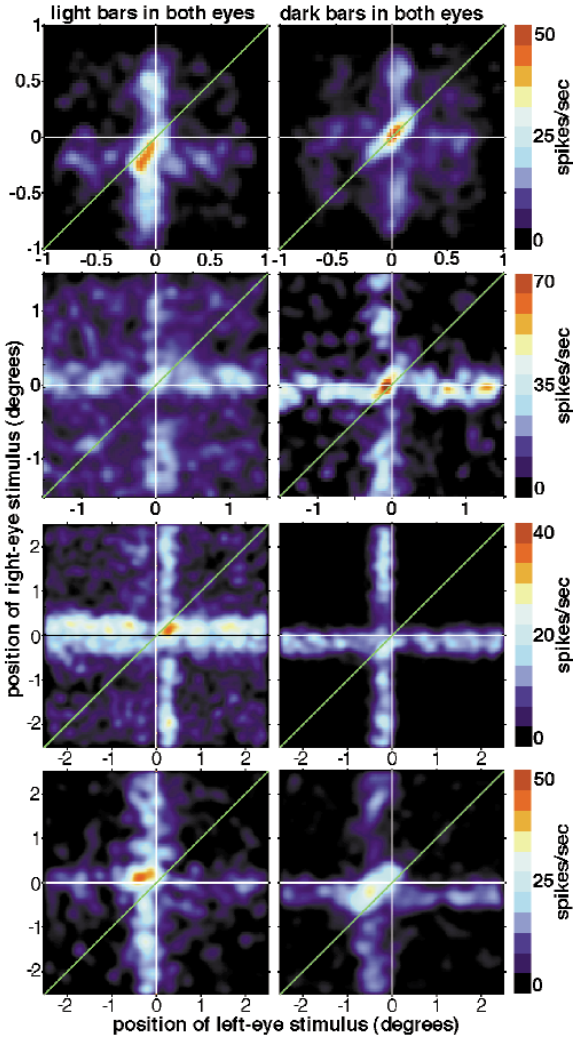

Fig. 6. Reverse-correlation binocular-response maps corrected for eye position for four cells with spatially offset light- and dark-excitatory response regions. Conventions as in Fig. 2. The top cell had a receptive field with a light-excitatory region lying to the left of a dark-excitatory region; in the three other cells, these regions were reversed. From the top, the receptive-field eccentricities were 2°, 5°, 14° and 9°.

surprisingly showed a larger spatial offset between light and dark-bar regions in one eye than in the other (as in **Fig. 5**). The disparity-tuned cells shown in Fig. 6 had spatially segregated light and dark excitatory subregions in both eyes. Nonetheless, the region of maximal binocular response was diagonally elongated, indicating position-invariant disparity selectivity. Thus a linear (or squared or rectified) sum of the monocular maps does not predict actual binocular responses. Therefore it is not clear whether these spatially segregated cells were simple or complex. Here we refer to cells that showed a spatial offset between light and dark excitatory regions that was larger than half the subunit width at half height as 'spatially offset'. Like the disparity-tuned complex cells, disparity-tuned, spatially offset cells also had binocular response maps with a diagonally elongated peak response region oriented at about 45° (**Fig. 4**), indicating position-invariant disparity selectivity.

For the population of cells with spatially offset light and dark regions, the spatial offset of the peaks in the two eyes' receptive-field maps usually roughly corresponded to the disparity tuning (**Fig. 7a**). The regression slope for the spatially offset cells was 0.9; therefore, on average the magnitude of the disparity preference correlated with offset of the peaks in the monocular receptive fields. We cannot determine from our data whether the monocular receptive-field offsets in spatially offset cells were generated by phase or positional offsets. Complex cells, with spatially overlapping light and dark response zones, also sometimes showed spatial offsets in the peaks of the two eyes' receptive fields, but showed a weaker correlation between the actual disparity preference and the offsets of the monocular peaks (regression slope, 0.4).

We examined the relative frequencies of facilitatory or suppressive binocular interactions in these disparity-tuned cells (compared with the linear prediction). For both light-bar and dark-bar stimuli for each cell, we calculated the maximum response facilitation and maximum response suppression from the binocular nonlinear interaction maps, and expressed the difference as a fraction of the maximum response for that bar/contrast condition (**Fig. 7b**). All cells showed suppressive interactions, and many cells showed facilitatory interactions; however, facilitation and suppression were neither negatively nor positively correlated.

Discussion

We found that both complex cells and cells with spatially offset ON and OFF subregions showed position-invariant disparity selectivity. The finding that spatially offset cells showed position-invariant disparity selectivity suggests that their disparity selectivity is wired up in a specific manner, rather than arising from random variations in the subunit organization between the two eyes. Moreover, the finding that the non-stereo-tuned cells showed round binocular interaction peaks, rather than being elongated along random axes, also suggests that there is something quite specific about the wiring of the disparity-tuned cells.

Some complex cells in anesthetized cat V1 show position-invariant bands in their binocular-interaction maps[9,10]. Furthermore, some simple cells show phase offsets between the two eyes' receptive fields, but Ohzawa and colleagues could not correlate these with disparity tuning in paralyzed animals[19,20]. They proposed that complex cells inherit disparity selectivity from a series of simple cells with the same disparity selectivity but different receptive field positions. Their model, combining disparity-tuned simple cells using a squaring nonlinearity, can account for complex cell behavior. Our binocular response maps of primate complex cells resembled those of the cat; however, we also found position-invariant disparity selectivity in cells with spa-

© 1999 Nature America Inc. • http://neurosci.nature.com

© 1999 Nature America Inc. • http://neurosci.nature.com

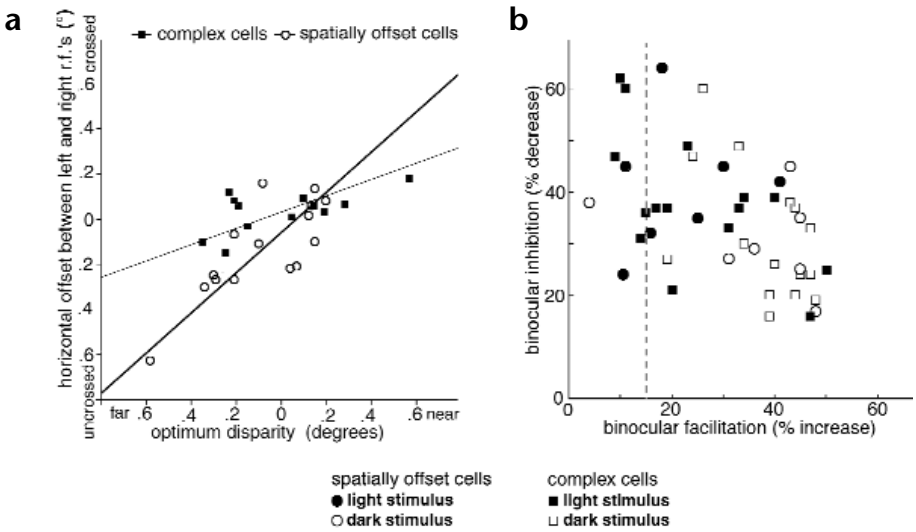

Fig. 7. (a) Optimum horizontal disparities (determined from binocular response maps) as functions of spatial offset of the peaks in the two eyes' receptive fields for complex cells and for spatially offset cells. For both variables, light- and dark-bar responses were averaged together. Filled squares indicate complex cells; open circles indicate spatially offset cells. **(b)** Scatter plot of facilitation versus suppression in 20 cells with clear monocular maps. We calculated the maximum response facilitation and maximum response suppression in the binocular non-linear interaction maps for each cell for both light-bar stimuli and dark-bar stimuli. These differences were expressed as fractions of the maximum responses for each bar/contrast condition. Dotted lines indicate two average standard deviations of the backgrounds outside the binocular region of the binocular non-linear interaction maps.

© 1999 Nature America Inc. • http://neurosci.nature.com

tially offset ON and OFF subregions. Indeed, we found no disparity-tuned cells whose binocular-interaction profiles could be described as a simple consequence of their monocular receptive fields and that could therefore serve as the building block for disparity selectivity. It is of course possible that we may have missed a large population of disparity-tuned simple cells for some reason, so we cannot absolutely rule out their existence in the monkey.

Those cells we observed with spatially offset light and dark excitatory subregions, but with a diagonal band of binocular interaction, must be in some sense complex because of their position-invariant disparity selectivity, which is a nonlinearity. Similarly, some direction-selective cells in the primate also showed the simple-like qualities of spatial segregation of excitatory and inhibitory subregions without spatial segregation of light and dark subregions[23]. This is consistent with previous studies. Others found few disparity-tuned simple cells in primate[15–17], and simple cells are rare outside layer 4C regardless of whether they are disparity tuned[26–30]. In anesthesized cat, by contrast, position-invariant disparity selectivity was found in binocular interaction maps of 8 of 49 simple cells[31]; like us, these researchers were unsure as to whether to call these simple cells or not, so they referred to them as "simple cell-like complex cells". However, their simple cells were selected only for binocularity, whereas our population was selected for disparity selectivity. As they had no way of determining zero disparity, it is possible that many of their simple cells peaked at zero disparity, and therefore would not have been considered disparity tuned. Therefore the "simple cell-like complex cells" may have been the only simple cells in the cat study that would qualify as disparity selective by our criteria, and the monkey and the cat could be quite similar, after all.

Because we failed to find any simple cells with disparity selectivity derived from receptive-field offset, we considered other models that compute disparity selectivity directly on the dendrites. Koch and Poggio[32] and Mel and colleagues[33] have proposed two different mechanisms for dendritic computation of disparity selectivity. Koch and Poggio's model supposes that excitatory inputs from one eye can be 'vetoed' by more proximal inhibitory inputs from the opposite eye, an 'AND–NOT' operation. The model proposed by Mel and colleagues involves facilitatory nonlinearities[33]; they also show that various types of active channels in the dendrite, such as calcium spikes, sodium spikes or NMDA receptors, could result in synergy between nearby synaptic inputs[34,35]. Therefore, if each dendrite samples a specific region of the visual field in each eye, with a systematic relationship between the visual-field locations in the two eyes, this model can generate position-invariant binocular facilitation. Suppressive bands at nonoptimal disparities could arise if the monocular inputs have inhibitory flanks. For cells tuned to nonzero disparities, both models would require some kind of systematic offset between interacting right- and left-eye inputs. Mel and colleagues proposed that this kind of local offset might arise by a learning mechanism[33], but it could also arise by a systematic offset in the dendritic sampling of the retinotopic maps for the two eyes; such an offset might be reflected in an overall receptive-field offset between the two eyes, as we observed (**Fig. 7a**).

Methods

Recordings. Recording techniques and reverse-correlation mapping with correction for eye position have been described[23]. Briefly, two male rhesus macaque monkeys were implanted with head posts, recording chambers and eye coils under sterile conditions[36,37].

We recorded extracellularly with fine electropolished tungsten electrodes coated with vinyl lacquer (Frederick Haer, Bowdoinham, Maine). Extracellularly recorded signals were amplified, bandpass filtered (1–10 kHz) and fed into a dual-window discriminator (BAK Electronics, Germantown, Maryland). Only well-isolated single units were used for mapping. We usually recorded from two units simultaneously using two electrodes and amplifiers. A Gateway 2000 90 MHz Pentium computer was used for stimulus generation and data collection. Stimuli were presented on a 21-inch NEC multisynch monitor with a 72 Hz refresh rate (non-interlaced), and the monitor screen was 100 cm in front of the monkey. The eye-position monitor was manufactured by DNI (Newark, Delaware). The monitor showed 0.05° peak-to-peak noise while recording the monkey's eye position. The monitor was calibrated before and after each recording session by having the monkey look at dots in the center and the four corners of the monitor.

Color-separation filters and colored stimuli were used to stimulate each eye independently and to generate stimuli at different interocular disparities. The energies of the phosphors were adjusted so that the luminance of the red phosphor through the red filter was the same as the luminance of the blue and green phosphors through the cyan filter. Light stimulus luminance through filters was 3.7 cd per m^2, with < 6% light leakage between stimuli for the two eyes.

© 1999 Nature America Inc. • http://neurosci.nature.com

For each single unit tested, we first determined the optimal orientation and then used moving bars of that orientation to determine the disparity tuning. For the first few cells in this study, maps and disparity tuning were obtained with the filters alternately reversed to confirm that colors we used did not affect the binocular-interaction map or the disparity tuning by themselves, which they did not.

Mapping technique. As outlined in Fig. 1e, monocular receptive fields and binocular interactions were mapped simultaneously using a modification[23] of the binocular-interaction[9,10] reverse-correlation technique[22]. The monkey was rewarded with a drop of juice for keeping its gaze within 1–2° of a continuously present 0.05° fixation spot for 3–4 seconds. Pairs of optimally oriented bars (one for each eye) were presented simultaneously along a dimension perpendicular to the cell's preferred orientation. Data shown here were collected using stimulus durations of 42 or 56 ms, with 42 or 56 ms between stimuli. Each stimulus position along the stimulus range was determined by a random-number generator. Data were collected at 0.03° resolution and were smoothed with a 0.15° Gaussian along both axes. A continuous record was kept of left eye position (at four-ms resolution), each stimulus position and spike occurrences (at one-ms resolution). Then data were read back as stimulus position relative to eye position (retinal location of stimulus) at a given delay before each spike. The optimum delay for each map was taken as the time to peak of the poststimulus response histogram (40–100 ms).

During mapping, we tried to center the stimulus range over each cell's receptive field. The position labeled 0 on the vertical and horizontal axes in each map represents the center of the stimulus range, and is usually near the center of the receptive field. The position of the receptive field with respect to the horizontal and vertical axes is, therefore, somewhat arbitrary. However, the location of the green diagonal is not arbitrary; it represents zero disparity—the plane of the monitor on which the monkey was fixating.

Light stimuli were presented on a black background, and dark stimuli on a light background. We did not use light and dark bars on an intermediate-luminance background because the higher contrast bars gave the strongest, most reproducible and clearest maps. To reduce frequency of large changes in the background luminance, responses to light-on-dark or dark-on-light stimuli were interspersed in sets of trials several minutes in duration rather than on a trial-by-trial basis; data were not collected for the first minute after each background change to allow the spontaneous firing to approach a steady state. At least three sets of each configuration were presented interspersed with other stimulus configurations, and data were rejected if there was any shift or change in the maps from the first to the last set. Each map represents at least 2500 spikes.

We presented stimuli over a large-enough region of the visual field that stimuli at either extreme were outside the cell's activating region. Therefore the monocular receptive-field profiles could be determined by averaging unsmoothed responses near the edges of the binocular response maps. We then calculated the linear predicted binocular interaction by simply summing the two monocular maps, corrected for background firing. Binocular nonlinear interaction maps were then calculated by subtracting this linear sum from the actual binocular response maps, and the difference was expressed as a fraction of the maximum response for that bar/contrast condition. These binocular nonlinear interaction maps are theoretically equivalent to the those obtained by Ohzawa *et al.*[10] by subtracting the opposite-contrast maps from the same-contrast maps. (Our method does not require obtaining all four maps, which can be limiting in an alert animal.) How well our calculation works can be seen from the fact that the binocular nonlinear interaction maps are near zero everywhere except in the middle, where significant binocular interactions are observed.

Optimum disparity was calculated by measuring horizontal distance from zero disparity of the peak in the smoothed binocular response map and multiplying it by the cosine of the angle of the stimulus. To determine if a cell was spatially offset, receptive-field widths were measured by averaging the unsmoothed monocular responses and taking the height at half of the peak, and that width was compared with the spatial offset of the peaks in the light and dark maps; cells were considered spatially offset if the light/dark peak offset was larger than half the average peak width at half height.

Offsets between the peaks in two eyes' receptive fields (**Fig. 7a**) were measured by smoothing the monocular maps and finding the peak position. For complex cells, monocular profiles were averages of the light- and dark-bar responses; for spatially offset cells, dark-bar responses were subtracted from light-bar responses. The distance (in horizontal visual space) between the peaks of these profiles for the two eyes was taken as the receptive-field offset.

Spatial resolution of the mapping technique. Because the presence of diagonal bands in binocular response maps suggests something fundamental about the way disparity is coded, we must consider how diagonal bands might arise artifactually. First, could the diagonal bands be produced by monitoring and correcting for the position of only one eye? For the maps obtained in this study, eye position was recorded for only the left eye. One monkey used in this study had eye coils in both eyes; the standard deviation of the difference between the two eye positions measured in this monkey as it performed the same fixation task in separate experiments was 7.8 minutes of arc, small compared to the measured binocular interactions and in agreement with previous measurements[38]. Moreover, constant, small, eye movements, for which we correct, are convergent in the two eyes (D.Y.T. and David Hubel, unpublished observations). We felt, therefore, that mapping with respect to one eye position should give high resolution. Nonetheless, if vergence eye movements (movement of unmonitored eye relative to the monitored eye) occurred, then these movements would add a random disparity signal to our calculation, which would tend to cancel out rather than artifactually generate any disparity-specific bands. Vergence errors could only cause diagonal bands in disparity space if disparity preference varied systematically with vergence; this does not seem to occur[39].

The second potential source of error is inadequate compensation for binocular, conjugate eye movements; failure to accurately compensation for conjugate eye movements might produce artifactual diagonal bands in the binocular-interaction maps. For example, if the response to two eyes is larger than the response to either eye alone, then a diagonal band of enhanced binocular responses would fall along the zero-disparity diagonal if conjugate eye movements were uncompensated. Therefore, nonconjugate eye movements (and the fact that we monitor only one eye) are not likely to artifactually generate disparity selectivity in our maps, but inadequately compensated conjugate eye movements might. (Note that such artifacts are also possible in anesthetized paralyzed preparations, because residual eye movements could also be conjugate and produce the artifactual appearance of position-invariant disparity selectivity.) It is therefore important to determine how accurately we can map small receptive fields in alert monkeys. The resolution of our eye-movement monitor is 0.05°, but a number of factors, such as spatial nonlinearities in the monitor, spikes occurring during saccades and vergence eye movements could affect the accuracy with which we compensated for eye position changes. We therefore simply asked how small a receptive field we could resolve.

We recorded cells with receptive-field widths as narrow as 0.2°, and cells with clear segregation of ON and OFF subunits at eccentricities as small as 4–6°. Maps of some of these cells can be seen on the *Nature Neuroscience* web site (http://neurosci.nature.com/supplementary_info/). Even for small receptive fields, the right-eye maps are not less precise than the left-eye maps, indicating that, at least during these mapping sessions, monkeys generally maintained gaze at a constant vergence, presumably fixating on the plane of the monitor.

The fact that we can resolve subunits of some receptive fields does not rule out the possibility that there are much smaller subunits that we cannot resolve, and it does not guarantee that our technique gives such high resolution every day, although eye-monitoring calibrations were consistent between the beginning and end of each recording session and from day to day, so there is no reason to suspect that resolution varies over time.

In some cases, we tentatively assigned a recorded cell to a layer based solely on physiological criteria[16,23,26,40]. In many cases, cells were recorded in the roof of the calcarine sulcus, where the transition from white matter to layer 6 is particularly clear from the receptive-field displacement.

These studies were carried out in accordance with NIH and Harvard Medical School guidelines and were approved by the Harvard Medical School Standing Committee on the Use of Animals.

Note: Response maps of cells can be found on the Nature Neuroscience web site (http://neurosci.nature.com/supplementary_info/).

© 1999 Nature America Inc. • http://neurosci.nature.com

© 1999 Nature America Inc. • http://neurosci.nature.com

ACKNOWLEDGEMENTS

This work was funded by NIH grant EY10203. David Freeman did the computer programming. Gail Robertson provided technical assistance. Clay Reid, Bevil Conway, Terrence Sejnowski, Rajesh Rao, Niall McLoughlin, Bartlett Mel and Tomaso Poggio provided suggestions on the manuscript.

RECEIVED 14 JUNE; ACCEPTED 14 JULY 1999

1. Wheatstone, C. Contributions to the physiology of vision—part the first. On some remarkable, and hitherto unobserved phenomena of binocular vision. *Phil. Trans. R. Soc. (Lond.)* **128**, 371–394 (1838).
2. Barlow, H. B., Blakemore, C. & Pettigrew, J. D. The neural mechanism of binocular depth discrimination. *J. Physiol. (Lond.)* **193**, 327–342 (1967).
3. Nikara, T., Bishop, P. O. & Pettigrew, J. D. Analysis of retinal correspondence by studying receptive fields of binocular single units in cat striate cortex. *Exp. Brain Res.* **6**, 353–372 (1968).
4. Pettigrew, J. D., Nikara, T. & Bishop, P. O. Binocular interaction on single units in cat striate cortex: simultaneous stimulation by single moving slit with receptive fields in correspondence. *Exp. Brain Res.* **6**, 391–410 (1968).
5. Joshua, D. E. & Bishop, P. O. Binocular single vision and depth discrimination. Receptive field disparities for central and peripheral vision and binocular interaction on peripheral single units in cat striate cortex. *Exp. Brain Res.* **10**, 389–416 (1970).
6. Bishop, P. O., Henry, G. H. & Smith, C. J. Binocular interaction fields of single units in the cat striate cortex. *J. Physiol. (Lond.)* **216**, 39–68 (1971).
7. Fischer, B. & J. Krüger, J. Disparity tuning and binocularity of single neurons in the cat visual cortex. *Exp. Brain. Res.* **35**, 1–8 (1979).
8. Ferster, D. A comparison of binocular depth mechanisms in areas 17 and 18 of the cat visual cortex. *J. Physiol. (Lond.)* **311**, 623–655 (1981).
9. Ohzawa, I. DeAngelis, G. C. & Freeman, R. D. Stereoscopic depth discrimination in the visual cortex: neurons ideally suited as disparity detectors. *Science* **249**, 1037–1041 (1990).
10. Ohzawa, I., DeAngelis, G. C. & Freeman, R. D. Encoding of binocular disparity by complex cells in the cat's visual cortex. *J. Neurophysiol.* **77**, 2879–2909 (1997).
11. Hubel, D. H. & Wiesel, T. N. Stereoscopic vision in macaque monkey. Cells sensitive to binocular depth in area 18 of the macaque monkey cortex. *Nature* **225**, 41–42 (1970).
12. Poggio, G. F., Doty, R. W. Jr. & Talbot, W. H. Foveal striate cortex of behaving monkey: single-neuron responses to square-wave gratings during fixation of gaze. *J. Neurophysiol.* **40**, 1369–1391 (1977).
13. Clarke, P. G., Donaldson, I. M. & Whitteridge, D. Binocular visual mechanisms in cortical areas I and II of the sheep. *J. Physiol. (Lond.)* **256**, 509–526 (1976).
14. Pettigrew, J. D. & Konishi, M. Neurons selective for orientation and binocular disparity in the visual Wulst of the barn owl (*Tyto alba*). *Science* **193**, 675–678 (1976).
15. Poggio, G. F. & Fischer, B. Binocular interaction and depth sensitivity in striate and prestriate cortex of behaving rhesus monkey. *J. Neurophysiol.* **40**, 1392–1405 (1977).
16. Poggio, G. F., Gonzales, F. & Krause, F. Stereoscopic mechanisms in monkey visual cortex: binocular correlation and disparity selectivity. *J. Neurosci.* **8**, 4531–4550 (1988).
17. Poggio, G. F. Mechanisms of stereopsis in monkey visual cortex. *Cereb. Cortex* **3**, 193–204 (1995).
18. Hubel, D. H. & Wiesel, T. N. Receptive fields, binocular interaction and functional architecture in the cat's visual cortex. *J. Physiol. (Lond.)* **160**, 106–154 (1962).
19. Ohzawa, I., DeAngelis, G. C. & Freeman, R. D. Encoding disparity by simple cells in the cat's visual cortex. *J. Neurophysiol.* **75**, 1779–1805 (1996).
20. Anzai, A., Ohzawa, I. & Freeman, R. D. Neural mechanisms underlying binocular fusion and stereopsis: position vs. phase. *Proc. Natl. Acad. Sci. USA* **94**, 5438–5443 (1997).
21. Qian, N. Binocular disparity and the perception of depth. *Neuron* **18**, 359–368 (1997).
22. Jones, J. P. & Palmer, L. A. The two-dimensional spatial structure of simple receptive fields in cat striate cortex. *J. Neurophysiol.* **58**, 1187–1211 (1987).
23. Livingstone, M. S. Mechanisms of direction selectivity in macaque V1. *Neuron* **20**, 509–526 (1998).
24. Cumming, B. G. & Parker, A. J. Responses of primary visual cortical neurons to binocular disparity without depth perception. *Nature* **389**, 280–283 (1997).
25. Movshon, J. A., Thompson, I. D. & Tolhurst, D. J. The receptive-field organization of complex cells in the cat's striate cortex. *J. Physiol. (Lond.)* **283**, 79–99 (1978).
26. Livingstone, M. S. & Hubel, D. H. Anatomy and physiology of a color system in the primate visual cortex. *J. Neurosci.* **4**, 309–356 (1984).
27. Hubel, D. H. & Wiesel, T. N. Receptive fields and functional architecture of monkey striate cortex. *J. Physiol. (Lond.)* **195**, 215–243 (1968).
28. Schiller, P. H., Finlay, B. L. & Volman, S. F. Quantitative studies of single-cell properties in monkey striate cortex. I. Spatiotemporal organization of receptive fields. *J. Neurophysiol.* **39**, 1288–1319 (1976).
29. Blasdel, G. G. & Fitzpatrick, D. Physiological organization of layer 4 in macaque striate cortex. *J. Neurosci.* **4**, 880–895 (1984).
30. Gonzalez, F., Alonso, J. M., Relova, J. L. & Perez, R. Receptive field asymmetries and sensitivity to random dot stereograms. *Arch. Ital. Biol.* **134**, 169–184 (1996).
31. Anzai, A., Ohzawa, I. & Freeman, R. D. Neural mechanisms for processing binocular information. I. Simple cells. *J. Neurophysiol.* (in press).
32. Koch C. & Poggio, T. in *Synaptic Function* (eds. Edelman, G. M., Gall, W. E. & Cowan, W. M.) 637–685 (Wiley, New York, 1987).
33. Mel, B. W., Ruderman, D. L. & Archie, K. A. in *Advances in Neural Information Processing Systems* Vol. 10 (eds. Jordan, M. I., Kearns, M. J. & Solla, S. A.) 208–214 (MIT Press, Cambridge, Massachusetts, 1998).
34. Mel, B. W., Ruderman, D. L. & Archie, K. A. Translation-invariant orientation tuning in visual "complex" cells could derive from intradendritic computations. *J. Neurosci.* **18**, 4325–4334 (1998).
35. Mel, B. W. Synaptic integration in an excitable dendritic tree. *J. Neurophysiol.* **70**, 1086–1101 (1993).
36. Wurtz, R. H. Visual receptive fields of striate cortex neurons in awake monkeys. *J. Neurophysiol.* **32**, 727–742 (1969).
37. Judge, S. J. *et al.* Implantation of magnetic search coils for measurement of eye position: an improved method. *Vision Res.* **20**, 535–538 (1980).
38. Motter, B. C. & Poggio, G. F. Binocular fixation in the rhesus monkey: spatial and temporal characteristics. *Exp. Brain Res.* **54**, 304–314 (1984).
39. Trotter, Y. *et al.* Modulation of neural stereoscopic processing in primate area V1 by viewing distance. *Science* **257**, 1279–1282 (1992).
40. Snodderly, D. M. & Gur, M. Organization of striate cortex of alert, trained monkeys (*Macaca fascicularis*): ongoing activity, stimulus selectivity, and widths of receptive field activating regions. *J. Neurophysiol.* **74**, 2100–2125 (1995).

© 1999 Nature America Inc. • http://neurosci.nature.com